Seismic Studies during the JARE South Pole Traverse 1968-69

*Tsuneo ETO**

1. Introduction

During the 1968-69 austral summer, the JARE South Pole Traverse party undertook a program of seismic investigation of the ice cap in the East Antarctic plateau area.

Throughout the traverse, an attempt was made to measure the ice thickness at 27 stations by seismic reflection shootings at approximately 100 km intervals. Though reflection shootings yielded poor records, they are now being analysed. The phenomenon of prolonged surface noise on cold firn after the detonation was the major obstacle to unequivocal sounding of the ice cap.

Refraction profiles were shot at five stations to determine variation in the velocity of seismic waves with depth in the upper transition zone from snow to ice. Velocity variations over the area are also of interest for the study of densification of the snow.

2. Seismic Equipments

The seismic equipments used on this traverse were the same instruments used in the JARE traverse 1967-68, Syowa-Plateau Station. Seismic equipments were as follows.

2.1. Geo-Space Model III amplifier system

A master case having 12 amplifier channels was used. This amplifier system is designed to amplify and control reflection and refraction seismic signals for recording on magnetic tape and recording oscillograph.

2.2. Geo-Space AM 200 magnetic recording system

The AM 200 field recording system provides a record and playback facilities for recording seismic data on a standard Techno type 7.24″×24.568″ AM tape.

2.3. Geophone

Each of the 12-channel amplifier was activated by a vertically oriented geophones having a natural frequency of 20 cps. The 12 geophones were normally spaced 20 m apart, giving a total spread of 220 m across the snow surface. Geophones were each provided with a stout spike pushed into the snow.

2.4. Camera

Geo-space DRO 6-28-X recording oscillograph with Du Pont's LINO-WRIT

* Sakura-jima Volcanological Observatory, Kyoto University, Sakura-jima, Kagoshima. Member of the JARE South Pole Traverse 1968-69.

MRK 376 direct writing paper was used. Type G, 9″ FL 200 cps galvanometers were used with an optical system to obtain photographic recordings.

2.5. Spread cable

Light weight "Vector" cables were used, comprising 13 pairs of conductors each going to one of the take-out, the latter being spaced at 20 m intervals. One end of cables was fitted with a plug and the other with a socket. The cables and geophones were mounted on a small sledge.

2.6. Explosives

"Nitratron" primer manufactured by the Nippon Oils & Fats Co., Ltd., was used. All of the "Nitratron" primer were in 500-g tins which could be screwed together to increase charge weights. The detonators were ordinary seismic ones, with leads 20 m long and made by the Teikoku Kakoohin Mfg. Co., Ltd.

2.7. Shot-hole auger

The auger was a device primarily intended for the glaciologist to take snow core samples of 8 cm in diameter. It is usually known as SIPRE core drill. This auger has a core barrel 1 m long, and drill rods of 1 m length which can be added successively as the hole deepens. A team of three or four men could drill to 10-m depth in about 3 hours.

As much as possible, the seismic instruments were mounted inside the snow vehicle KD606, but spares, explosives, shot-hole auger, and the small sledge with cables and geophones were carried on sledges.

3. Seismic Velocity Determination

The seismic measurements consisted of short refraction profiles to ascertain near-surface velocity structure and long refraction shots (up to about 1.2 km) to measure the velocity of propagations of compressional P waves in the snow.

Travel time curves were prepared for five long refraction stations (example

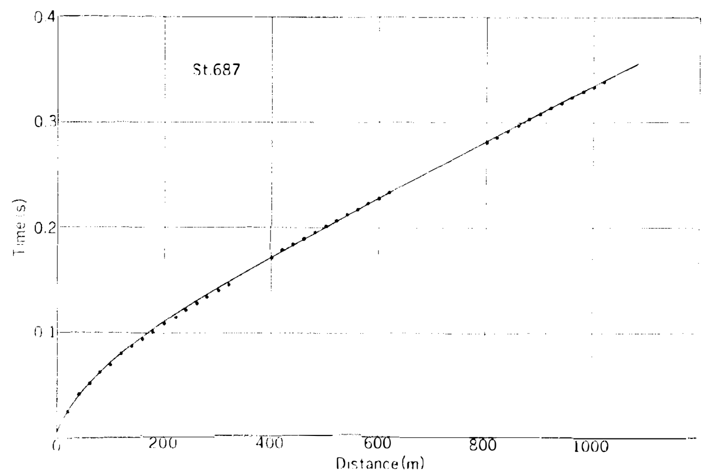

Fig. 1. Travel time curve for refraction at St. 687.

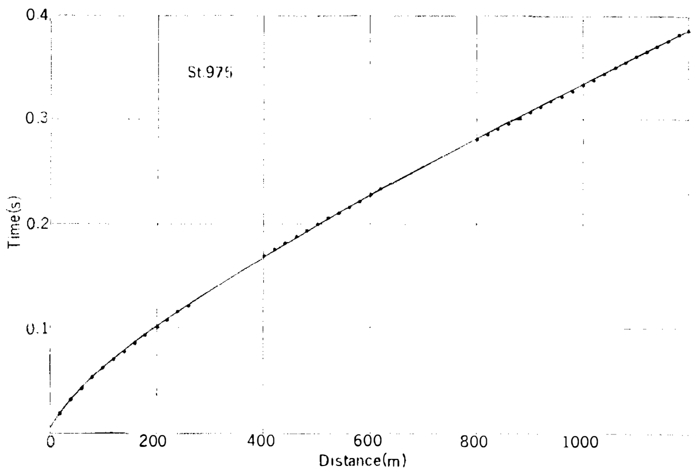

Fig. 2. Travel time curve for refraction at St. 975.

in Figs. 1 and 2) from which velocity variations with distance were measured.

Assuming a continuous increase of velocity with depth, as described by SLICHTER (1932), velocity-distance curves were reduced to velocity-depth curves by the standard Weichert-Herglotz-Bateman formula,

$$Z_{x_1}=\frac{1}{\pi}\int_{x=0}^{x=x_1}\cosh^{-1}\left(\frac{V_{x_1}}{V_x}\right)dx$$

where, V_{x_1} is the instantaneous velocity obtained at a distance x_1 from the shot point and Z_{x_1} is the depth below the snow surface where this velocity occurs. Rays from the shot point to a geophone proceed by curving paths. The velocity V_{x_1} with which the arrivals move along the spread at x_1 is equal to the velocity of the waves at the deepest point Z_{x_1} on the ray. The arrival velocity V_{x_1} used were picked from the travel time curve at intervals out to a distance of about 1.2 km by laying a tangent to the curve. The depth Z_{x_1} is found as the integral of a function of the arrival velocity V_{x_1} over all distances from zero to x_1, the emergent distance of the ray whose greatest depth is being investigated.

By numerical integration of these data, using the above formula, the velocity variation to depths of about 230 m was calculated. The maximum velocity is reached at about 220 m below the snow surface. Data for five refraction stations during the traverse are given in Tables 1-5 and in Figs. 3-6.

4. Snow Densification

From the compressional seismic wave velocity with depth values calculated for five refraction stations, snow density with depth profiles was calculated, using the empirical expression which ROBIN (1958) showed to be valid below the depth of 15 m.

$$\rho=2.21\times10^{-4}\left(\frac{1}{1-0.00061T}\right)V_p+0.059$$

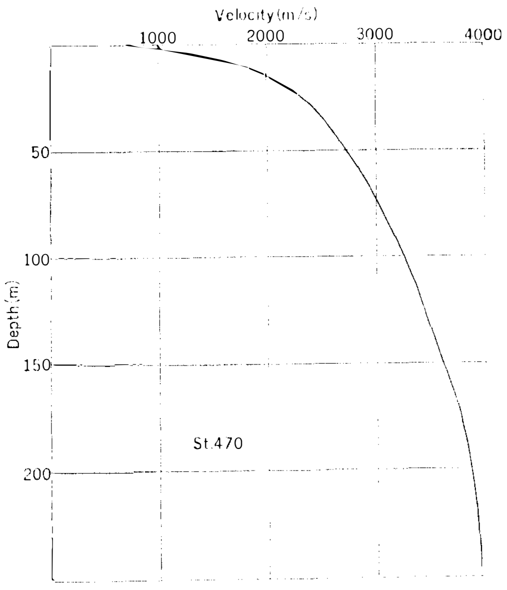

Fig. 3. Velocity-depth profiles at St. 470.

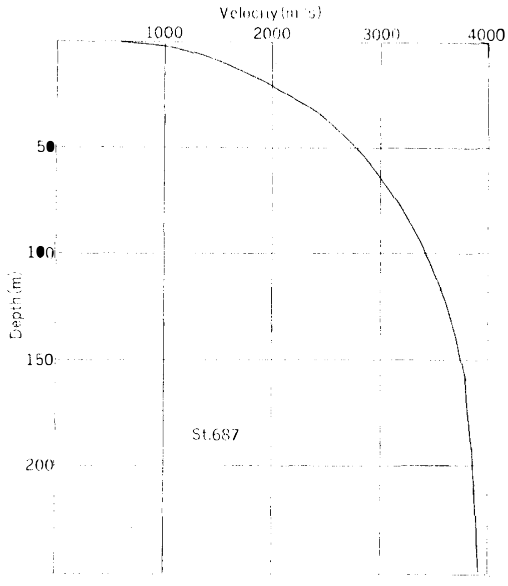

Fig. 4. Velocity-depth profiles at St. 687.

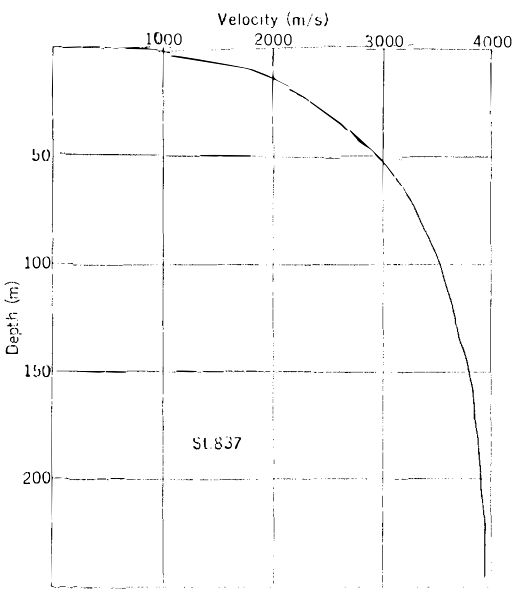

Fig. 5. Velocity-depth profiles at St. 837.

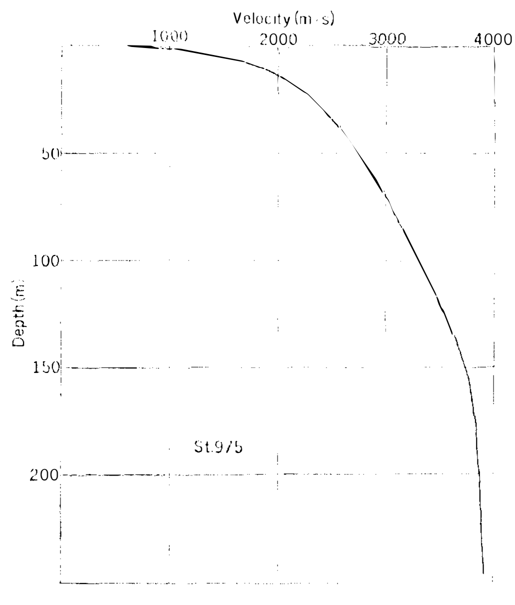

Fig. 6. Velocity-depth profiles at St. 975.

where, ρ is snow density (g/cm^3), V_p is P wave velocity (m/s), and T is the temperature (°C).

The results of these calculations using the snow temperature of about 10-m depth are also tabulated in Tables 1-5.

Table 1. Distance-velocity-depth and density profiles at St. 470.

Horizontal distance (m)	Velocity (m/s)	Depth (m)	Density (g/cm^3)
0	885	0	—
10	1,196	1.9	—
20	1,389	4.2	—
30	1,613	7.1	—
40	1,675	9.3	—
50	1,776	11.9	—
60	1,905	14.8	0.467
70	2,114	18.4	0.511
80	2,198	21.1	0.529
90	2,278	23.7	0.546
100	2,359	26.6	0.564
120	2,457	31.4	0.583
140	2,488	35.5	0.591
160	2,506	39.7	0.595
180	2,551	44.2	0.605
200	2,632	49.3	0.622
220	2,688	54.0	0.634
240	2,695	58.0	0.636
260	2,710	62.1	0.639
280	2,725	66.2	0.642
300	2,763	70.7	0.650
350	2,933	86.0	0.687
400	3,145	99.0	0.732
450	3,345	113.8	0.775
500	3,390	124.2	0.784
550	3,484	136.4	0.804
600	3,636	151.3	0.837
650	3,677	160.9	0.846
700	3,759	173.0	0.863
750	3,788	183.2	0.869
800	3,831	193.9	0.879
850	3,861	204.2	0.885
900	3,906	215.0	0.895
950	3,937	225.4	0.901
1,000	3,937	231.4	0.901

Table 2. Distance-velocity-depth and density profiles at St. 556.

Horizontal distance (m)	Velocity (m/s)	Depth (m)	Density (g/cm³)
0	585	0	—
10	1,006	2.2	—
20	1,198	4.6	—
30	1,374	7.2	—
40	1,550	9.9	—
50	1,672	12.4	—
60	1,859	15.4	0.456
70	1,980	18.0	0.482
80	2,151	21.4	0.518
90	2,315	24.4	0.553
100	2,500	27.7	0.593
120	2,604	31.9	0.615
140	2,703	36.4	0.636
160	2,786	40.5	0.654
180	2,857	44.7	0.669
200	2,865	48.0	0.671
220	2,882	51.4	0.674
240	2,907	55.1	0.680
260	2,950	59.1	0.689
280	2,976	62.7	0.695
300	3,068	67.5	0.714
350	3,125	76.6	0.726
400	3,175	85.7	0.737
450	3,257	95.5	0.755
500	3,333	105.2	0.771
550	3,413	115.2	0.788
600	3,460	124.5	0.798
650	3,496	133.2	0.804

Table 3. Distance-velocity-depth and density profiles at St. 687.

Horizontal distance (m)	Velocity (m/s)	Depth (m)	Density (g/cm³)
0	588	0	—
10	1, 060	2. 6	—
20	1, 271	5. 2	—
30	1, 414	7. 9	—
40	1, 538	10. 5	—
50	1, 698	13. 4	—
60	1, 862	16. 6	0. 457
70	2, 053	19. 9	0. 498
80	2, 212	23. 1	0. 532
90	2, 283	25. 6	0. 547
100	2, 326	27. 8	0. 556
120	2, 381	32. 1	0. 568
140	2, 558	37. 8	0. 606
160	2, 681	42. 9	0. 632
180	2, 770	47. 5	0. 651
200	2, 907	53. 0	0. 680
220	2, 985	57. 6	0. 697
240	3, 021	61. 6	0. 705
260	3, 058	65. 7	0. 713
280	3, 096	69. 8	0. 721
300	3, 125	73. 8	0. 727
350	3, 236	84. 5	0. 751
400	3, 345	95. 5	0. 774
450	3, 484	107. 2	0. 804
500	3, 559	117. 4	0. 820
550	3, 610	127. 2	0. 831
600	3, 663	137. 0	0. 842
650	3, 704	146. 6	0. 851
700	3, 745	156. 2	0. 859
750	3, 774	165. 5	0. 866
800	3, 817	175. 2	0. 875
850	3, 831	184. 1	0. 878
900	3, 846	193. 0	0. 881
950	3, 861	201. 9	0. 884
1, 000	3, 891	211. 4	0. 891
1, 050	3, 922	220. 9	0. 897
1, 100	3, 937	229. 7	0. 900

Table 4. Distance-velocity-depth and density profiles at St. 837.

Horizontal distance (m)	Velocity (m/s)	Depth (m)	Density (g/cm³)
0	654	0	—
10	1,140	2.4	—
20	1,462	5.2	—
30	1,667	8.0	—
40	1,792	10.5	—
50	1,890	12.9	—
60	2,004	15.5	0.489
70	2,045	17.7	0.498
80	2,141	20.4	0.518
90	2,262	23.3	0.544
100	2,375	26.1	0.568
120	2,392	29.9	0.572
140	2,597	35.7	0.616
160	2,740	41.0	0.647
180	2,865	46.2	0.674
200	2,976	51.2	0.697
220	3,049	55.8	0.713
240	3,086	59.9	0.721
260	3,115	63.9	0.727
280	3,145	67.9	0.734
300	3,195	72.3	0.744
350	3,367	84.2	0.781
400	3,436	94.3	0.796
450	3,534	105.2	0.817
500	3,597	115.3	0.831
550	3,677	125.8	0.848
600	3,718	135.5	0.857
650	3,759	145.2	0.865
700	3,802	154.9	0.875
750	3,831	164.3	0.881
800	3,846	173.3	0.884
850	3,876	182.8	0.890
900	3,906	192.3	0.897
950	3,922	201.3	0.900
1,000	3,937	210.2	0.903
1,050	3,937	218.3	0.903

Table 5. Distance-velocity-depth and density profiles at St. 975.

Horizontal distance (m)	Velocity (m/s)	Depth (m)	Density (g/cm^3)
0	599	0	—
10	1, 183	2. 7	—
20	1, 555	5. 6	—
30	1, 733	8. 2	—
40	1, 887	10. 7	—
50	1, 972	13. 1	—
60	2, 123	15. 8	0. 515
70	2, 183	18. 0	0. 527
80	2, 242	20. 3	0. 540
90	2, 288	22. 5	0. 550
100	2, 331	24. 7	0. 559
120	2, 381	28. 8	0. 570
140	2, 463	33. 3	0. 587
160	2, 545	37. 8	0. 605
180	2. 632	42. 5	0. 624
200	2, 732	47. 3	0. 645
220	2, 817	52. 1	0. 663
240	2, 841	56. 0	0. 669
260	2, 849	59. 7	0. 670
280	2, 890	63. 9	0. 679
300	2, 933	68. 2	0. 688
350	3, 049	79. 2	0. 713
400	3, 236	92. 0	0. 753
450	3, 322	102. 6	0. 772
500	3, 460	114. 5	0. 801
550	3, 521	124. 6	0. 815
600	3, 636	136. 4	0. 839
650	3, 677	146. 0	0. 848
700	3, 745	156. 5	0. 863
750	3, 802	166. 6	0. 875
800	3, 831	175. 9	0. 881
850	3, 846	184. 8	0. 884
900	3, 861	193. 7	0. 887
950	3, 876	202. 7	0. 891
1, 000	3, 891	211. 5	0. 894
1, 050	3. 891	220. 0	0. 894
1, 100	3, 891	228. 3	0. 894
1, 150	3, 891	236. 8	0. 894

References

ROBIN, G. de Q. (1958): Seismic shooting and related investigations. Scient. Results Norw.-Br.-Swed. Antarct. Exped. 1949–1952, **5** (Glaciology, III), 48–80.

SLICHTER, L. B. (1932): The theory of the interpretation of seismic travel-time curves in horizontal structure. Physics, **3**, 273–295.